Journal of Colloid and Interface Science 325 (2008) 324–330

Contents lists available at ScienceDirect

Journal of Colloid and Interface Science

www.elsevier.com/locate/jcis

Association (micellization) and partitioning of aglycon triterpenoids

Marjan Rafat [a], Kit Wah Fong [a], Arthur Goldsipe [b], Brian C. Stephenson [b], Samuel T. Coradetti [a], T.G. Sambandan [a], Anthony J. Sinskey [c], ChoKyun Rha [a,*]

[a] Biomaterials Science and Engineering Laboratory, Massachusetts Institute of Technology, 77 Massachusetts Ave, Cambridge, MA 02139, USA
[b] Department of Chemical Engineering, Massachusetts Institute of Technology, 77 Massachusetts Ave, Cambridge, MA 02139, USA
[c] Department of Biology, Massachusetts Institute of Technology, 77 Massachusetts Ave, Cambridge, MA 02139, USA

ARTICLE INFO

Article history:
Received 28 March 2008
Accepted 19 May 2008
Available online 3 June 2008

Keywords:
Surface activity
Partition coefficient
Solubility
Asiatic acid
Madecassic acid
CMC
Triterpenoids
Aggregation number
Molecular dynamics

ABSTRACT

Micellization and solution properties of the aglycon triterpenoids asiatic acid (AA) and madecassic acid (MA) were examined experimentally and in computational simulations. AA and MA belong to the large class of bioactive aglycon triterpenoids, for which limited physicochemical data are available. In this study, solubility, partition coefficient, critical micelle concentrations (CMC), and surface tensions of AA and MA were measured. Reverse phase HPLC data, supported by dye probe experiments and drop shape analysis, showed the CMC in phosphate buffered saline (PBS) to be 15 ± 2 μM, and 86 ± 9 μM for AA and MA, respectively. The surface tensions of AA and MA in PBS were 64.1 and 64.4 mN/m, respectively. Matrix-assisted laser desorption/ionization (MALDI) mass spectrometry indicated the aggregation numbers of AA and MA to be 5 to 7. Molecular dynamics simulations confirmed that molecular association could occur between 5 and 7 molecules in solution. The IC_{50} of AA and MA on human small cell carcinoma and human glioblastoma cell lines was 25 ± 5 μM and 66 ± 13 μM, respectively. The IC_{50} is within the range of calculated CMC of AA and MA in bioassay media, suggesting that the micellar aggregates may lead to their cytotoxicity.

1. Introduction

Over 4000 aglycon triterpenoids have been isolated from various plants and many have been suggested to have therapeutic applications, including anti-inflammatory and wound-healing properties [1,2]. Surprisingly, many biochemical mechanisms of bioactivity for these compounds have been proposed in the literature, without full consideration of their fundamental properties (e.g. solubility, partition coefficient, and critical micelle concentration, etc.). This is particularly notable because many aglycon triterpenoids contain hydrophobic and hydrophilic regions, which therefore might associate to form micelles or soluble aggregates.

While many of these compounds have been identified, obtaining large quantities of them in sufficient purity for experimentation is often difficult and time consuming. Furthermore, these compounds are mainly soluble in organic solvents or in organic/aqueous media, complicating the application of many ordinary techniques for physicochemical analysis that require mainly aqueous media. To address these problems, a reverse phase HPLC (RP-HPLC) procedure was developed to determine CMC. The procedure requires only a few milligrams of aglycon triterpenoid sample in organic/aqueous media.

Asiatic acid (AA) and madecassic acid (MA) are the most common aglycon triterpenoids of the commercially and traditionally popular medicinal herb *Centella asiatica*. They are frequently used for various therapeutic effects. Extracts such as TECA (titrated extract of *Centella asiatica*) [1] and dried aerial parts of these plants are available over the counter as therapeutics, frequently with the claim that their bioactive principles are triterpenoids such as AA or MA. Recent studies have also suggested that AA may have wide ranging multi-functional effects [3] and may even be an apoptotic anti-cancer agent [4–7], further bolstering claims of *Centella asiatica*'s medicinal properties.

AA and MA have chemical structures that are similar to those of bile acids well known surface active agents in physiological systems [8]. Bile acids, have a tetracyclic "steroid" skeleton, while AA and MA are pentacyclic [9]. These compounds are also semi-rigid, containing both hydrophobic and hydrophilic segments grouped mostly on opposite sides of the molecule (Fig. 1) [10,11]. The structural parallels between bile acids and aglycon triterpenoids suggest that the latter may also be surface-active and self-assemble into micelles.

The critical micelle concentration (CMC), partition coefficient, and solubility of AA and MA were determined. Molecular dynamics simulations complimented these experiments by modeling the

* Corresponding author. Fax: +1 617 253 6358.
E-mail address: ckrha@mit.edu (C.K. Rha).

0021-9797/$ – see front matter
doi:10.1016/j.jcis.2008.05.046

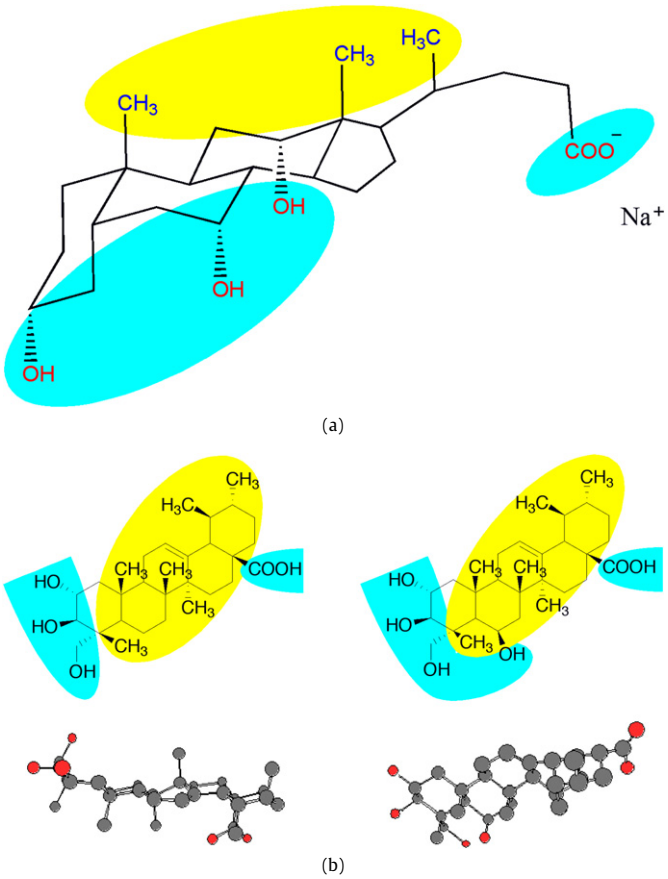

Fig. 1. (a) Structure of a bile salt [37]; (b) Structures of asiatic (left) and madecassic acid (right). The three-dimensional structures were obtained by energy minimization using Chem 3D Ultra (CambridgeSoft, Cambridge, MA, USA).

aggregation and interactions of these molecules in solution. IC_{50} were also determined on human small cell carcinoma (DMS114) and human glioblastoma cells (HTB-14) to compare to CMC. This is the first study to report the solution and partition behaviors of AA and MA.

2. Experimental

2.1. Reagents and solutions

AA and MA samples were provided by MMP Inc. (International Development and Manufacturing, South Plainfield, NJ, USA). The purity and identity of the samples were confirmed by analytical HPLC and MS. Samples were further purified to better than 99% purity by semi preparatory HPLC. Phosphate Buffered Saline solution (1 × PBS, pH 7.2, Mediatech, Herndon, VA) was used in all experiments. All other chemicals were reagent grade (Mallinckrodt, St. Louis, MO).

2.2. Solubility

Calibration curves for the solubility were constructed from RP-HPLC data. AA and MA samples were prepared by serial dilution of a stock solution of known concentration in methanol. The saturated solutions of AA and MA were made in phosphate buffered saline (PBS) and shaken overnight. Each saturated solution was centrifuged, and 1 mL of the supernatant was diluted to 10 mL with methanol. The concentration of the diluted solution (and hence the solubility) was determined by RP-HPLC using a calibration curve constructed by analysis of known concentrations of standard triterpenoid solutions.

2.3. Partition coefficient (log *K*)

Partition coefficients were determined [12] by dissolving 1 mg of AA or MA in 1 mL of octanol and 1 mL water. The solution was then shaken overnight. Both the upper and lower liquid phases were analyzed by RP-HPLC to determine the quantity of AA and MA in each phase. The partition coefficient was calculated by computing the ratio of the concentration in octanol to the that in water [13,14] as determined by HPLC peak areas. The hydrophobic–lipophilic balance (HLB) of each triterpenoid was estimated using the software Molecular Modeling Pro (Norgwyn Montgomery Software, North Wales, PA).

2.4. Reverse phase analytical HPLC assay

Solutions of various concentrations below and above the CMC of AA and MA were made in methanol, PBS, or 1% DMSO/ethanol in PBS. Each 20 µL sample was passed through an HPLC system (D-7000 HPLC System, Hitachi Instruments, Inc., San Jose, CA) at 210 nm with a 5 µm, 100 A, 150 mm L × 3.19 mm ID Delta-PAK C4 column (Waters, Milford, MA) at a flow rate of 1 mL/min. The mobile phase was 0.05% H_3PO_4 in water (A) and acetonitrile (B). A gradient table was developed for separation of compounds. The peak area versus triterpenoid concentration was plotted. Each solution was prepared using serial dilutions of stock solutions in designated solvents.

2.5. Preparatory HPLC procedure for purification

Solutions containing compounds were further purified with an HPLC system (Polaris System, Varian Inc., Palo Alto, CA) with a Platinum EPS C18 column, 10 µm, 250 mm L × 10 mm ID (Altec, Deerfield, MI). The compounds were eluted with a gradient system: 0.1% TFA in water (solvent A) and acetonitrile (solvent B), at a flow rate of 5 mL/min and detected at 210 nm. Heart cut fractions were collected and lyophilized to obtain the purified compound as a dry, white, powder of greater than 99% purity.

2.6. Drop shape analysis

Surface tensions and CMC were determined by the drop volume method [15–17]. Saturated solutions of AA and MA were made in PBS. AA or MA solutions were prepared by diluting the supernatant from a saturated stock solution. The diluted concentrations of AA or MA were selected to ensure that measurements were made at concentrations both below and above the CMC. Samples were loaded onto a syringe and analyzed by a G10/DSA10 Drop Shape Analysis System (Kruss GmbH, Hamburg, Germany) to determine the surface tensions. Measurements were taken after the drops equilibrated for 5 min.

2.7. Dye probe method with Nile red

The absorption of AA and MA with Nile red in PBS was measured at 220 nm with a UV spectrophotometer (Beckman DU 530 Life Science, Fullerton, CA). Each sample containing 3 mM Nile red was shaken overnight. The optical densities (OD) at 590 nm were measured for several dilutions of AA and MA.

2.8. Aggregation number

The aggregation numbers for AA and MA were estimated using matrix assisted laser desorption ionization (MALDI) spec-

troscopy [18]. The spectra of the solutions were obtained at concentrations between the CMC and saturation. MALDI spectra were taken with 2,5-dihydroxybenzoic acid (DHB) as the matrix. Equal volumes of the AA and MA solutions in water and the matrix solutions were mixed. The final solution in 1 μL quantity was directly deposited onto the sample holder. The masses of the aggregates obtained by MALDI (Voyager-DE STR) were divided by the mass of a singly charged molecule to estimate the aggregation number.

2.9. Molecular dynamics simulation

Simulations were conducted using a 2006 developers' version of the GROMACS software [19,20]. AA and MA were simulated at an all-atomistic level of detail using the OPLS-AA force field [21]. The carboxylate group of each molecule was treated as being fully dissociated, giving each monomer a net charge of −1. Sodium ions were added to solution as needed to preserve electroneutrality. Water was simulated explicitly using the simple extended point-charge model (SPC/E) [19]. Atomic charges were assigned for each molecule based on the default atomic charge values specified in the OPLS-AA force field.

Van der Waals interactions were treated using a cutoff distance of 9.0 Å, and Coulombic interactions were described using 3D particle mesh Ewald (PME) summation. A long range dispersion correction was applied to more accurately estimate the energy and pressure of the system. The Van der Waals cutoff chosen has been shown to be accurate for the OPLS-AA force field with the inclusion of long-range dispersion corrections [22–24]. In modeling short-ranged non-bonded interactions, a neighbor list of 9.0 Å was maintained and updated every 10 steps. Each simulation was carried out using fixed bond lengths, which permitted an increase in simulation timestep from 1 fs to 2 fs. Bond lengths were constrained using the SHAKE algorithm as implemented in GROMACS [25].

Simulations were conducted in the NPT (constant number of particles, constant pressure, and constant temperature) ensemble. In each simulation, the cell temperature was maintained at 298.15 K using a Berendsen temperature coupling algorithm, which mimics weak coupling to an external heat bath with first-order kinetics [26]. A Berendsen pressure coupling algorithm was applied to maintain each box at the specified pressure of 1.0 bar [26].

2.10. Molecular dynamics simulation: System preparation

Twenty-five nanosecond simulations were conducted for three different initial configurations of AA and MA. In each initial configuration, five AA or MA molecules were placed in aqueous solution. The initial size of all six simulation cells was 4 nm × 4 nm × 4 nm. Approximately 2000 water molecules were added to the AA and MA in each simulation cell. Five sodium counterions were also added to each simulation cell to make the solution electroneutral. To provide a more physically realistic initial configuration, these counterions were added by replacing the water molecules experiencing the greatest electrostatic potential. The potential was recalculated after every ion insertion.

In the first two initial configurations a micelle of MA or AA was preformed and then solvated. In the first of these (Configuration 1) the micelle was preformed by aligning 5 molecules parallel to the *z*-axis and placing them in close proximity. Because each monomer in this configuration had the same orientation, each of the negative charges in AA and MA were in relatively close proximity. In the second initial configuration (Configuration 2) the micelle was formed with the longest axis of each molecule oriented radially outwards from the micelle's center of mass. Each molecule was oriented such that its negatively charged carboxylate group was located at the outer edge of the micelle.

Table 1
Solubility of asiatic acid and madecassic acid in PBS

Triterpenoids	Solubility	
Asiatic acid	15.0 μg/mL	(30.6 μM)
Madecassic acid	85.0 μg/mL	(168.3 μM)

Table 2
Partition coefficients of asiatic acid and madecassic acid

	$\log_{10} K$ (calculated)	$\log_{10} K$ (experimental)	HLB
Asiatic acid	4.3	5.8	5.5
Madecassic acid	3.1	3.0	6.0

To ensure that extended simulations of preformed AA and MA micelles do not merely represent metastable states for the molecules in aqueous solution, we conducted a third simulation for AA and MA where the initial state was a random configuration of the monomers in water (Configuration 3).

After preparation of each AA and MA system, long simulation runs were conducted to evaluate the stability of the two preformed micelles and to observe whether self-assembly of randomly distributed AA and MA molecules in solution would occur. After performing an energy minimization to remove any close contacts between atoms, each system was simulated for 25 ns.

2.11. Biological assays

Human small cell lung carcinoma (NCI #DMS114) and human glioblastoma cell lines (ATCC #HTB-14) were obtained from the National Cancer Institute (Bar Harbor, ME) and the American Type Culture Collection (Rockville, MD), respectively. The cells were cultured in RPMI 1640 supplemented with 5% fetal bovine serum, penicillin and streptomycin at 37 °C in humidified air containing 5% carbon dioxide.

Cells were plated in a 24 well ELIZA plate at an initial density of 2×10^5 cells with 1.0 mL medium per well. Twenty-four hours after seeding, the medium was replaced with predetermined doses of AA or MA. The DMSO concentration in the culture medium was 0.1%. The cells were grown for 72 h. Cell viability was measured by the tetrazolium salt 3-(4,5-dimethylthiazol-2-yl)-2,5-diphenyl tetrazolium bromide (MTT) [27]. The experiments were made in quadruplicate.

All experiments were carried out at room temperature.

3. Results

3.1. Solubility

AA and MA are pentacyclic triterpenoids. These compounds have 3 or 4 hydroxyl groups and one carboxylic group; thus, AA and MA were expected to be somewhat soluble in aqueous solutions. However, experimentally, saturation is reached at low concentrations for both triterpenoids. The concentrations of AA and MA in dilutions of the supernatant of saturated solutions in PBS gave the solubilities of AA and MA to be 15 μg/mL or 31 μM and 85 μg/mL or 170 μM, respectively (Table 1).

3.2. Partition coefficients

The partition coefficients of AA and MA were calculated (http://www.molinspiration.com) and are presented in Table 2 along with experimental values and the calculated hydrophobic and lipophilic ratio (HLB). These values indicate that AA and MA are lipophilic with higher solubility in organic solvents. The chemical structures of AA and MA are similar, except that AA has three hydroxyl groups

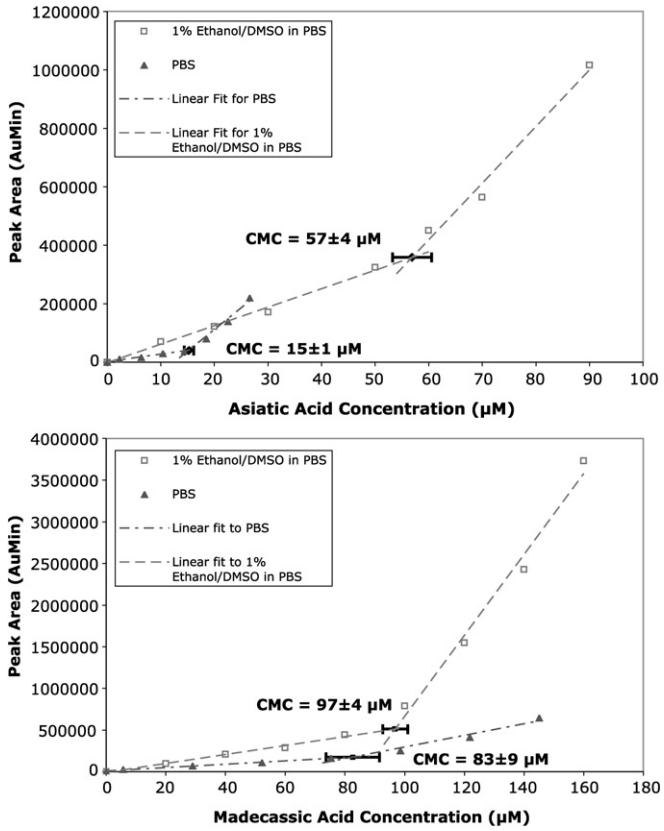

Fig. 2. HPLC calibration curves for asiatic acid in PBS and 1% DMSO/EtOH in PBS (top) and madecassic acid in PBS and 1% DMSO/EtOH in PBS (bottom).

while MA has four hydroxyl groups. The effect of the additional hydroxyl group of MA is reflected in its lower partition coefficient as well as its higher HLB. Because of the similarity of their chemical structures, AA and MA are predicted to have partition coefficients that differ by approximately one order of magnitude. However, the experimentally measured partition coefficients differ by nearly three orders of magnitude despite such a small difference in structure. This difference may be due to steric effects not accounted for in the predictive model. For example, small changes in the number or position of hydroxyl groups on a bile salt can change its partition coefficient by several orders of magnitude [12].

3.3. Reverse phase HPLC assay

The CMCs of AA and MA solutions were determined by RP-HPLC. Shaw and Elliott [28] describe an RP-HPLC method for determining the CMC whereby monomers and micelles each have distinct retention times. However, in our measurements, we did not observe two distinct peaks above the CMC but only a single peak. We discovered a break in the linearity of the HPLC area curve of the single observed peak. The breaks in the calibration curves of peak area versus concentration represent CMC and are in agreement with the CMC of AA and MA as determined by other experiments (i.e. drop shape analysis and the dye probe method). Fig. 2 depicts the effect of increasing concentrations of AA and MA in PBS and in 1% DMSO/EtOH in PBS. In all cases, a break in linearity is evident at CMC. For AA, the breakpoints occur at 15 ± 1 µM in PBS and 57 ± 4 µM in 1% DMSO/EtOH in PBS. For MA, the breakpoints occur at 83 ± 9 µM in PBS and 97 ± 4 µM in 1% DMSO/EtOH in PBS. The breakpoints coincide with the CMC in those particular solvent compositions. The CMC was also measured in aqueous media, and the results for all solvent compositions are given in Table 3.

Table 3
Experimentally determined CMC

Experimental method	Solvent	CMC	
		Asiatic acid (µM)	Madecassic acid (µM)
RP-HPLC	H_2O	16 ± 2	61 ± 8 (pH 5.65)
RP-HPLC	PBS	15 ± 1	83 ± 9
RP-HPLC	1% DMSO/ethanol in PBS	57 ± 4	97 ± 4
UV–VIS	PBS (3 mM Nile red)	15 ± 2	89 ± 9
DSA	PBS	19 ± 4	80 ± 10

Table 4
Estimated CMC for asiatic acid in various concentrations of DMSO in PBS solution

% DMSO	Calculated CMC	% DMSO	Calculated CMC
0.1	19–20 µM	0.6	39–40 µM
0.2	23–24 µM	0.7	41–43 µM
0.3	26–27 µM	0.8	45–47 µM
0.4	31–32 µM	0.9	48–51 µM
0.5	35–36 µM	1.0	52–54 µM

The variations in the observed breakpoints in differing solvents again indicate that the CMC is sensitive to the nature or composition of the solvent, particularly for AA. Organic compounds like DMSO have been shown to increase the CMC of common surfactants [29]. Table 4 shows the estimated CMC of AA in PBS solutions with DMSO/EtOH (interpolated from HPLC data at 0% and 1% DMSO/EtOH). Such solvent compositions are commonly used in biological assays. The consequent effect on CMC affects the resulting bioactivity and toxicity of AA.

3.4. Drop shape analysis

Fig. 3 shows that the surface tension decreases with increasing concentration of AA and MA. In each case, the surface tension drops abruptly to a minimum of approximately 64 mN/m. The CMC value is determined as the concentration at which the surface tension reaches this minimum. By this method, the CMC of AA and MA in PBS was measured to be approximately 19 ± 4 µM and 80 ± 10 µM, respectively. Drop shape analysis was performed to confirm the CMC and only a few concentrations were tested. The error in the measurements was 15% to 20%.

3.5. Dye probe method with Nile red

Using Nile red as a probe, the optical density (OD) of AA and MA at various concentrations in PBS was measured at 590 nm. A clear break was observed in the Beer–Lambert Law plot of OD versus AA/MA concentration (Fig. 4). This break indicates an increase in dye solubility due to AA/MA micelle formation. The CMCs for AA and MA in PBS were determined to be 15 ± 2 µM and 89 ± 9 µM, respectively.

3.6. Aggregation number

The micelle aggregation numbers were estimated using MALDI mass spectra of aggregates taken from solid-state samples. Singly charged species were obtained up to m/z 3000, corresponding to AA or MA (and sodium counterions) aggregation numbers between 3 and 7. The aggregation numbers of the most prominent peaks were found to be 5 and 6 for AA and MA, respectively. These experiments suggest that the uniform crystal aggregates formed in MALDI are representative of the molecules in solution.

3.7. Molecular dynamics simulation

Dynamic computational simulations of the stability and formation of micelles of AA and MA molecules in aqueous solution

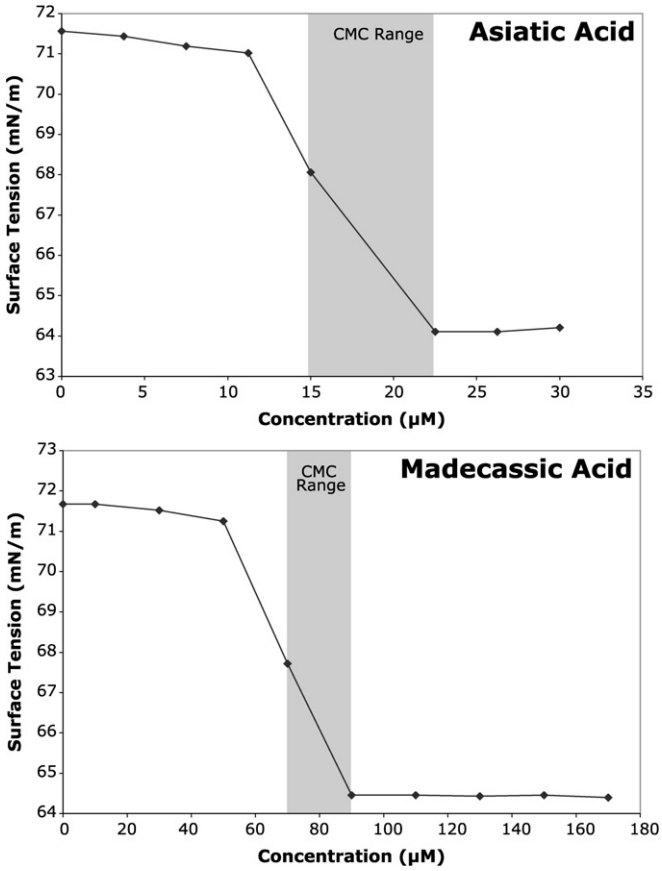

Fig. 3. Surface tension determined by drop shape analysis.

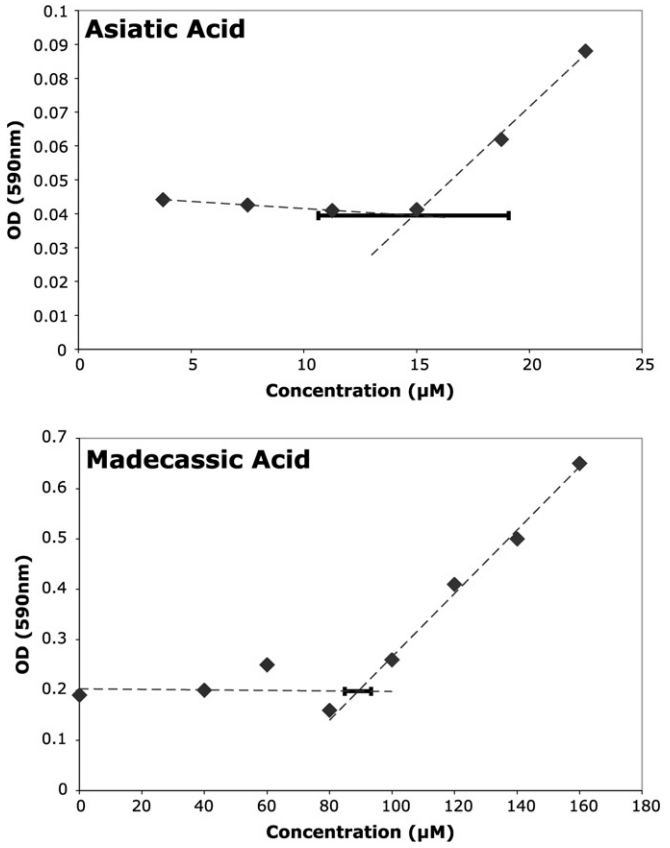

Fig. 4. CMC of asiatic acid (top) and madecassic acid (bottom) determined with Nile red.

provided further support for self-assembly or aggregation. A preformed AA micelle composed of five molecules with their long axes aligned in parallel (Configuration 1) was stable over a 25 ns simulation. Although significant fluctuations in the configuration of the micelle occurred, no AA molecules broke away from the micelle over the course of the simulation. A preformed AA micelle composed of five molecules with their long axes in a radial configuration (Configuration 2) initially broke up, indicating this starting configuration was not stable. However, after 9 ns, several of the AA molecules were observed to form clusters in solution, and they remained associated for the remainder of the simulation. In Configuration 3, five AA molecules were initially distributed randomly in solution. As early as 0.7 ns into the simulation, association between pairs of AA molecules was observed. After simulation for approximately 3 ns, the 5 monomers had self-assembled into a micellar structure. This micelle remained stable for the remainder of the 25 ns simulation. A snapshot of both the initial and final states of this third simulation (based on Configuration 3) is shown in Fig. 5.

The MA micelle formed with Configuration 1 was stable for the first 10 ns of simulation. At that point, two molecules of MA broke off from the original micelle. However, the remaining cluster of three MA molecules remained stable and was joined at 24 ns by one of the two MA molecules that had drifted into the aqueous solution. The MA micelle formed with Configuration 2 initially broke up, but reformed into a 5-monomer micelle after 6.5 ns of simulation. This newly formed micelle remained stable for the remaining 18.5 ns of simulation. When started from a random configuration in solution (Configuration 3), the MA molecules began to cluster after roughly 0.1 ns of simulation. All MA molecules assembled into a micelle after 16 ns of simulation, and this micelle remained stable for the remaining 9 ns of simulation. A snapshot of both the initial and final states of this third simulation (based on Conformation 3) is shown in Fig. 5.

3.8. Biological assays

AA and MA showed a dose-dependent inhibition of cell growth (Fig. 6). AA inhibited both type of cells at essentially the same IC_{50} (25 ± 5 μM). Further, MA also inhibited the cells at the same IC_{50} for each cell line (66 ± 13 μM). The results, summarized in Table 5, suggest that the cytotoxicity occurs around CMC; the viability of both cell lines decreased precipitously at the CMC. The CMC of AA and MA in the bioassay media (0.1–0.2% DMSO in PBS), as interpolated from HPLC data are estimated to be 19–24 μM (Table 4) and 70–90 μM, respectively. The solubility or partition characteristics of AA and MA may be the primary factor determining their cytotoxicity, rather than cell type.

4. Discussion

The solubility of MA in PBS, 168.3 μM, is approximately 6 times that of 30.6 μM for AA, despite only a slight structural difference (Table 1). The partition coefficients ($\log K$) in octanol and water for the two aglycon triterpenoids are given in Table 2 [14]. The values of the experimentally determined $\log K$, especially for AA (5.8), indicate that these aglycon triterpenoids are surface active. AA only differs from MA by one hydroxyl group, yet an increase of almost three orders of magnitude is observed in the experimental $\log K$ value. The HLB values indicate that they are wetting agents, likely facilitating bioactivity [30]. Their assembly at surfaces and interfaces and spontaneous organization in water into dynamic aggregates or micelles indicates that they may, in such a manner, participate in physical, biological, or physiological effects. The aggregation properties, such as micelle size and shape, ultimately

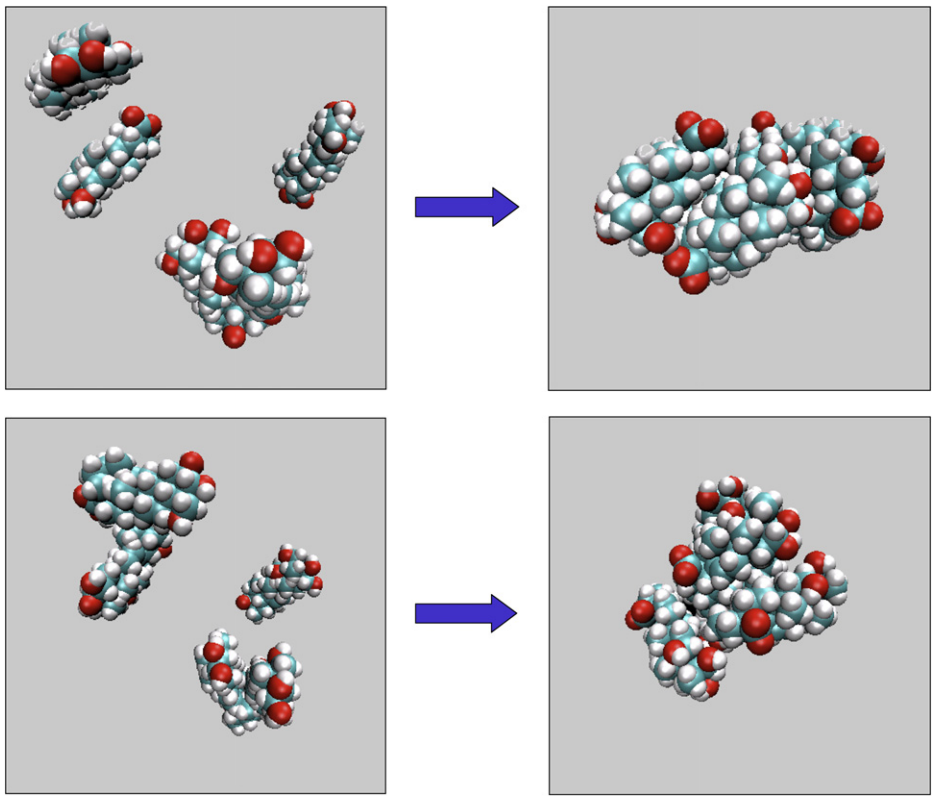

Fig. 5. Simulation results for asiatic acid and madecassic acid. Initial and final configurations of molecules of asiatic acid (top) and madecassic acid (bottom) after 25 ns of simulation in aqueous solution. The initial configuration was generated by placing 5 molecules randomly in a 4 nm × 4 nm × 4 nm simulation cell. Water molecules and sodium ions are not shown for clarity.

control overall bioactivity via monomer structure and concentration as well as the solution conditions.

The CMC of both AA and MA as determined by drop shape analysis was approximately 10% higher than the CMC determined by HPLC methods and the range of values was also greater (15% to 20%). Since the surface tension of the drop was measured after aging the drop for a finite time, equilibrium may not have been reached, and that may have caused the variation in experimental values [31].

RP-HPLC curves for concentration calibration of AA and MA in both PBS and 1% DMSO/EtOH in PBS displayed an evident break in linearity (Fig. 2). The observation of this break in the linearity of the HPLC peak area versus concentration calibration curve is not found in the literature and is a noteworthy discovery. Furthermore, it is interesting that in each case the break occurs at a concentration coincident with CMC. Therefore, the break in the linearity is indicative of the aggregation or association of molecules taking place in solution at this concentration. This discovery is of practical importance as HPLC calibration, which is a routine practice in many laboratories requiring a small quantity of test sample, may also be used to determine CMC. Each solvent caused the CMC to occur at different concentrations, indicating that differing solution conditions drive varying propensities for micelle formation [32].

Molecular dynamics simulations suggest that AA and MA form aggregates or micelles in aqueous solution and that they have similar aggregation behavior. High levels of fluctuation characterized both AA and MA micelles. Significant rearrangement within the micelles was observed over 25 ns of simulation for each system. In some cases the simulation time was sufficient to observe an exchange of AA and MA molecules between the micelle and bulk water [21].

The IC_{50} of AA and MA were found to be 25 ± 5 and 62 ± 12 μM, respectively, on human small cell carcinoma. They were 23 ± 5 μM and 71 ± 14 μM for MA and human glioblastoma cell lines (Fig. 6). These values were all found to occur near the estimated CMC (Table 5). Small cells of lung carcinoma were less lipophilic than glioblastoma cells. Nevertheless, IC_{50} for both cell lines were similar for both AA and MA. In bioassays with normal fibroblast cells, the IC_{50} also occurred near the CMC at 32 μM for AA and 67 μM for MA. Likewise, much of the literature on the bioactivity of these aglycon triterpenoids indicates that the IC_{50} for these compounds was found to be near the CMC value (Table 6) [4,6,7]. There are some significant discrepancies in reported IC_{50} in the literature. Differences in solvent composition, and thus different CMC, may be the cause of these discrepancies.

Significant decreases in viability starting near or above CMC suggest that the biological mechanisms of action should be considered in the context of the interaction between micelles and the cell membrane and consequent intracellular activity. Similar phenomena have been described with other micelle forming compounds. Podevin et al. [33] described the effect of bile salts on lymphocyte proliferation by claiming that the biological effect was partly due to the modification of the structure of the cell membrane lipid bilayer by the surface activity and hydrophobicity of bile salts. Similarly, Sudo et al. [34] described that succinolyl trehalose lipid-3 (STL-3) inhibited the growth of Human HL-60 cells at or near the CMC (4 μM). Morgan et al. (1998) [35] showed that bile salts (chenodeoxycholic acid) also decreased the viability of cultured kidney cells (MDCK and NRK) at the CMC (3 mM).

The bioactivity studies on AA reported in literature have not included the surface activity in the study of the biological mechanisms of action [1,4–7,36]. However, it has been observed that surface-active complexes show cytotoxicity at CMC. There is no question that the micellization and partitioning behavior of these aglycon triterpenoids are fundamental to their bioactivity.

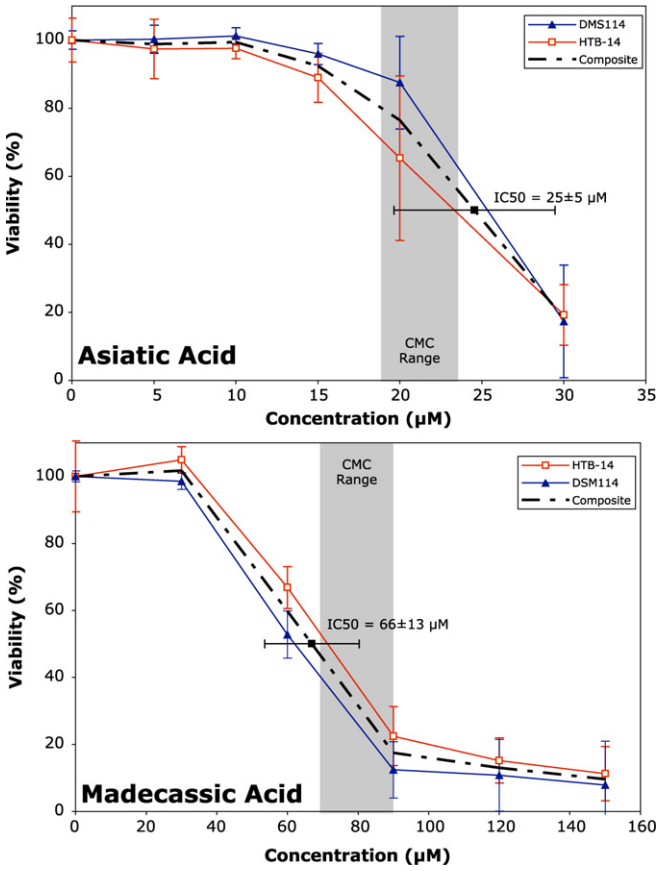

Fig. 6. IC_{50} of AA (top) and MA (bottom) on DMS114 and HTB-14 cell lines. The shaded area represents the approximate range of the CMC calculated for the medium.

Table 5
Cytotoxicity of asiatic acid and madecassic acid

Cell line	IC_{50} of asiatic acid (with 0.1% DMSO)	IC_{50} of madecassic acid (with 0.1% DMSO)
DMS114 (human lung cancer cell)	25 ± 5 μM	62 ± 12 μM
HTB-14 (human brain cancer cell)	23 ± 5 μM	71 ± 14 μM
CRL-2450 (human fibroblast)	32 μM	67 μM

Table 6
IC_{50} of asiatic acid (literature comparison)

Cell line	IC_{50}
HT-29[5] (human colon adenocarcinoma)	72 μM
HepG2[3] (human hepablastoma)	30 μM
SK-MEL-2[6] (human melanoma)	35 μM
U-87 MG[7] (human glioblastoma)	20–30 μM

5. Conclusions

1. The surface tensions of the aglycon triterpenoids AA and MA solutions at the CMC are 64 mN/m, as measured by drop shape analysis.
2. The CMC of AA and MA were evaluated by RP-HPLC, drop shape analysis and dye solubilization. The CMC is approximately 15 μM for AA and 83 μM for MA in PBS and varies with solvent conditions.
3. A break point in RP-HPLC peak area versus concentration calibration curves occurs at the CMC for AA and MA in various solvent compositions.
4. The aggregation number for AA and MA as determined by MALDI experiments is 5–7, which concurs with GROMACS simulation studies that show stable aggregation occurring at an aggregation number of 5.
5. The CMC may provide guidance for a first approximation of the cytotoxicity or bioactivity of AA and MA.

Acknowledgments

This study was supported in part by the Malaysia-MIT Biotechnology Partnership Program (MMBPP). We are grateful to Professor Alan Hatton for the use of his laboratory instruments. A. Goldsipe and B.C. Stephenson thank Professor Daniel Blankschtein for valuable discussion and guidance. We also thank Amanda Lanza for her participation in this research.

References

[1] F.X. Marquart, G. Bellon, P. Gillery, Y. Wegrowski, J.P. Borel, Connect. Tissue Res. 24 (2) (1990) 107.
[2] A.D. Widgerow, L.A. Chait, R. Stals, P.J. Stals, Aesthetic Plast. Surg. 24 (2000) 227.
[3] C. Cho, D. Choi, M. Cardone, C. Kim, A. Sinskey, C. Rha, Cell Biol. Toxicol. 22 (6) (2006) 393.
[4] Y.S. Lee, D.-Q. Jin, E.J. Kwon, S.H. Park, E.-S. Lee, T.C. Jeong, D.H. Nam, K. Huh, J.-A. Kim, Cancer Lett. 186 (1) (2002) 83.
[5] Y. Soo Lee, D.-Q. Jin, S.-M. Beak, E.-S. Lee, J.-A. Kim, Eur. J. Pharmacol. 476 (3) (2003) 173.
[6] P. Bunpo, K. Kataoka, H. Arimochi, H. Nakayama, T. Kuwahara, U. Vinitketkumnuen, Y. Ohnishi, J. Med. Invest. 52 (1–2) (2005) 65.
[7] B.C. Park, K.O. Bosire, E.-S. Lee, Y.S. Lee, J.-A. Kim, Cancer Lett. 218 (1) (2005) 81.
[8] W.N. Setzer, M.C. Setzer, Mini Rev. Med. Chem. 3 (6) (2003) 540.
[9] B. Sing, R.P. Rostogi, Phytochemistry 8 (1969) 917–921.
[10] D. Barret, S.H. Gellman, J. Am. Chem. Soc. 115 (1993) 9343.
[11] P. Venkatesan, Y. Cheng, D. Kahne, J. Am. Chem. Soc. 116 (1994) 6955.
[12] A. Roda, A. Minutello, M. Angellotti, A. Fini, J. Lipid Res. 31 (1990) 1433.
[13] R.A. Day, A.L. Underwood, Quantitative Analysis, Prentice–Hall, Englewood Cliffs, NJ, 1980.
[14] A. Berthod, S. Carda-Broch, J. Chromatogr. A 1037 (1–2) (2004) 3.
[15] T. Lohnstein, Ann. Phys. 325 (1906) 237.
[16] R. Miller, V.B. Fainerman, A.V. Makievski, M. Ferrari, G. Loglio, in: K. Holmberg (Ed.), Handbook of Applied Surface and Colloid Chemistry, Wiley, 2002, p. 225.
[17] M.A.B.H. Susan, A. Ishibashi, Y. Takeoka, M. Watanabe, Colloids Surf. B Biointerfaces 38 (3–4) (2004) 167.
[18] D. Bongiorno, L. Ceraulo, A. Ruggirello, V.T. Liveri, E. Basso, R. Seraglia, P. Traldi, J. Mass Spectrom. 40 (12) (2005) 1618.
[19] H.J.C. Berendsen, D. van der Spoel, R. van Drunen, Comput. Phys. Commun. 91 (1–3) (1995) 43.
[20] E. Lindahl, B. Hess, D. van der Spoel, J. Mol. Model. 7 (8) (2001) 306.
[21] W.L. Jorgensen, D.S. Maxwell, J. Tirado-Rives, J. Am. Chem. Soc. 118 (1996) 11225.
[22] M. Shirts, J.W. Pitera, W.C. Swope, V.S. Pande, J. Chem. Phys. 119 (11) (2003) 5740.
[23] M.R. Shirts, V.S. Pande, J. Chem. Phys. 122 (13) (2005) 134508.
[24] M. Shirts, Precise and Accurate Free Energies in Biomolecular Systems, Stanford University, Stanford, CA, 2005.
[25] J.P. Ryckaert, G. Ciccotti, H.J.C. Berendsen, J. Comput. Phys. 23 (1997) 327.
[26] D. van der Spoel, E. Lindahl, B. Hess, A. van Buuren, E. Apol, P. Meulenhoff, D. Tieleman, A. Sijbers, K. Feenstra, R. van Drunen, H.J.C. Berendsen, GROningen Machine for Molecular Simulations User's Manual, Groningen, The Netherlands, 2004.
[27] M.B. Hansen, S.E. Nielsen, K. Berg, J. Immunol. Methods 119 (2) (1989) 203.
[28] R. Shaw, W. Elliott, Lipids 13 (12) (1978) 971.
[29] L. Panda, G.B. Behera, J. Indian Chem. Soc. 62 (1985) 44.
[30] J.A. Quinn, in: Norgwyn Montgomery Software, North Wales, PA, 2003.
[31] C. Bilke-Krause, U. Ohlerich, H.L. Mohle, Dynamic Properties of Surfactants—The Basis for a Profound Understanding of Their Industrial Application, Kruss GmbH Wissenshcaftliche Laborgerate Kolb Distribution Ltd., 2003.
[32] S. Reis, C.G. Moutinho, C. Matos, B. de Castro, P. Gameiro, J.L.F.C. Lima, Anal. Biochem. 334 (1) (2004) 117.
[33] P. Podevin, L. Correia, C. Montet, F. Conti, C. Chéreau, Y. Calmus, R. Poupon, Eur. J. Clin. Invest. 31 (4) (2001) 367.
[34] T. Sudo, X. Zhao, Y. Wakamatsu, M. Shibahara, N. Nomura, T. Nakahara, A. Suzuki, Y. Kobayashi, C. Jin, T. Murata, K.K. Yokoyama, Cytotechnology 33 (1) (2000) 259.
[35] W.A. Morgan, Y. Dingg, P.H. Bach, Ren. Fail. 20 (3) (1998) 441.
[36] F.X. Maquart, F. Chastang, A. Simeon, P. Birembaut, P. Gillery, Y. Wegrowski, Eur. J. Dermatol. 9 (4) (1999) 289.
[37] P. Garidel, A. Hildebrand, K. Knauf, A. Blume, Molecules 12 (2007) 2292.